Published as: *Nat Struct Mol Biol*. 2010 December ; 17(12): 1500–1507.

H2A.Z nucleosomes enriched over active genes are homotypic

Christopher M. Weber[1,2], **Jorja G. Henikoff**[1], and **Steven Henikoff**[1,3]

[1] Basic Sciences Division, Fred Hutchinson Cancer Research Center, 1100 Fairview Avenue North, Seattle Washington 98109, USA

[2] Molecular and Cellular Biology Program, University of Washington, Seattle Washington 98195, USA

[3] Howard Hughes Medical institute, Fred Hutchinson Cancer Research Center, Seattle, Washington 98109, USA

Abstract

Nucleosomes that contain the histone variant H2A.Z are enriched around transcriptional start sites, but the mechanistic basis for enrichment is unknown. A single octameric nucleosome can contain two H2A.Z histones (homotypic) or one H2A.Z and one canonical H2A (heterotypic). To elucidate H2A.Z function, we generated high-resolution maps of homotypic and heterotypic *Drosophila* H2A.Z (H2Av) nucleosomes. Although homotypic and heterotypic H2A.Z nucleosomes map throughout most of the genome, homotypic nucleosomes are enriched and heterotypic nucleosomes are depleted downstream of active promoters and intron/exon junctions. The distribution of homotypic H2A.Z nucleosomes resembles that of classical active chromatin and shows evidence of disruption during transcriptional elongation. Both homotypic H2A.Z nucleosomes and classical active chromatin are depleted downstream of paused polymerases. Our results suggest that H2A.Z enrichment patterns result from intrinsic structural differences between heterotypic and homotypic H2A.Z nucleosomes following disruption during transcriptional elongation.

The eukaryotic genome is packaged into nucleosome core particles that consist of ~147 bp of DNA wrapped around an octamer of four core histone proteins: H2A, H2B, H3, and H4, which must be modified to facilitate access to DNA for active processes. Alterations to nucleosomes include remodeling, post-translational modifications, and replacement of resident histones with histone variants. Whereas the major canonical histones are expressed during S phase and package the newly synthesized DNA into nucleosomes, replacement histone variants are expressed from distinct genes throughout the cell cycle and have

---

Correspondence should be addressed to S.H., Phone: (206) 667-4515, FAX: (206) 667-5889, steveh@fhcrc.org.

ACCESSION #
GEO GSE21615.

AUTHOR CONTRIBUTIONS
C.M.W. performed the experiments, J.G.H. did the analysis, S.H. supervised the work, and C.M.W. and S.H. wrote the paper.

COMPETING FINANCIAL INTERESTS
The authors declare that there are no competing financial interests.

important functional roles1. For example, the universal histone variant H2A.Z is a minor variant that comprises only ~5–10% of major H2A2–4, yet H2A.Z is essential for viability in many organisms, including *Tetrahymena thermophila*5, *Xenopus laevis*6 *Mus musculus*7 and *Drosophila melanogaster*8. Despite extensive characterization, the role of H2A.Z in gene regulation has remained elusive.

Exchange of major H2A for variant H2A.Z within the nucleosome is mediated by the Swr1 ATPase complex9–11. Studies in *Saccharomyces cerevisiae* using H2A.Z chromatin immunoprecipitation (ChIP) coupled with microarray technology (ChIP-chip) found that H2A.Z nucleosomes are distributed throughout the genome but are enriched at gene promoters4. In *Drosophila* embryos, H2A.Z localizes in the proximity of ~85% of transcription start sites (TSS)12. Many studies have looked more closely at the localization of H2A.Z at promoters, and a conserved profile across eukaryotes has emerged. H2A.Z localizes to the strongly positioned +1 nucleosome downstream from the TSS and a few positioned nucleosomes further downstream, but is relatively depleted over gene bodies12–15. In both *S. cerevisiae* and mammals, H2A.Z is also enriched upstream of TSSs, although this enrichment is not seen in *Drosophila*, *Arabidopsis*, or *Schizosaccharomyces pombe*. The basis for differential H2A.Z localization is unknown.

H2A.Z arose early in eukaryotic evolution and has remained distinct from H2A ever since1. Relative to H2A, H2A.Z has an extended acidic patch, which alters the nucleosome surface to interactions with other proteins, and a different docking domain, which interacts with the $(H3/H4)_2$ tetramer within the core particle. H2A.Z and H2A also have drastically different L1 loops, which comprise the only interaction surface between the pair of H2A-H2B dimers that flank the $(H3\text{-}H4)_2$ core of the nucleosome16. Whereas both the H2A-H2A and the H2A.Z-H2A.Z interaction surfaces are tightly interlocked, the H2A.Z-H2A.Z interaction is more extensive. Also, it does not appear that the nucleosome core particle can accommodate an H2A-H2A.Z interaction without a structural clash. Nevertheless, subsequent studies have shown that heterotypic nucleosomes containing both H2A and H2A.Z form *in vitro*17, and *in vivo* are more abundant than homotypic (H2A.Z-H2A.Z-containing) nucleosomes18. *In vitro* studies have indicated that these different structural forms have different inherent properties. For example, reconstituted homotypic H2A.Z nucleosomes are relatively resistant to disruption by high ionic strength solutions19–21 and are refractory to RNA polymerase passage22. Furthermore, after acetylation, reconstituted homotypic H2A.Z nucleosomes are more stable than either heterotypic H2A.Z or canonical H2A nucleosomes23.

We wondered whether these different structural properties between canonical, heterotypic and homotypic nucleosomes might contribute to H2A.Z localization and function *in vivo*. Accordingly, we generated high resolution, genome-wide maps of heterotypic and homotypic H2A.Z nucleosomes in *Drosophila* S2 cells. We find that heterotypic and homotypic H2A.Z nucleosomes are distributed almost indistinguishably genome-wide. However, homotypic H2A.Z nucleosomes are highly enriched just downstream of TSSs of active genes, where heterotypic H2A.Z nucleosomes are relatively depleted, and are enriched downstream of intron/exon junctions. Homotypic H2A.Z nucleosomes also correspond closely to low-salt-soluble nucleosomes, and are depleted from genes regulated

by RNA Polymerase II (Pol II) pausing, where both are deficient. Our findings lead to a structure-based dynamic model that can help explain both H2A.Z localization and molecular function.

RESULTS

Distribution of homotypic and heterotypic H2Av nucleosomes

To separate heterotypic and homotypic H2A.Z nucleosomes, we used sequential affinity purification with two different tags on H2A-type histones. *Drosophila* has a single replication-independent H2A variant, H2Av, which functions both as H2A.Z and H2A.X24. *Drosophila* S2 cell lines that express biotin-tagged H2A (Biotag-H2A) or H2Av (Biotag-H2Av) histones were infected with baculovirus expressing FLAG-tagged H2Av driven by the inducible *Drosophila* metallothionein promoter (Supplementary Fig. 1). We prepared native micrococcal nuclease digested (MNased) chromatin from these two baculovirus-infected lines using a low-salt EDTA shearing protocol, which maximally solubilizes chromatin under minimally disruptive conditions25. We then fixed soluble nucleosomes consisting of mostly mononucleosomes with formaldehyde to ensure integrity of labile nucleosomes through subsequent purification steps. We isolated DNA from the tagged nucleosomes bound to streptavidin beads (Fig 1a–b), and sequenced the purified nucleosomal DNA using the paired-end mode of the Illumina Genome Analyzer (Supplementary Fig. 2). We also sequenced a fraction of the input from one heterotypic and one homotypic H2Av purification experiment, which consisted of mostly mononucleosomes. The sequenced input DNA displayed extensive genome-wide coverage (Fig 1c). Surprisingly, profiles from both heterotypic and homotypic H2Av nucleosomes also showed broad genome-wide distributions. Although both heterotypic and homotypic H2Av nucleosomes are nearly ubiquitous throughout the genome, quantitative differences were evident in comparing input, heterotypic, and homotypic H2Av nucleosomes. The close correspondence between biological replicates in each case indicates that these differences are robust. We also analyzed transposon families and found major differences in nucleosome density, as indicated by their very different transposon landscapes for input, heterotypic and homotypic nucleosomes (Supplementary Fig. 3a). However, we detected only slight differences between input, heterotypic, and homotypic H2Av nucleosomes within a family (Supplementary Fig. 3b). Therefore, H2Av nucleosomes of both types are broadly distributed throughout the *Drosophila* genome.

Homotypic H2Av nucleosomes are enriched downstream of TSSs

The sequencing of paired-end libraries precisely maps particles that are protected from MNase digestion, so that the integrity of the fragments used to generate libraries can be ascertained by bulk analysis of the fragment sizes that result. For each sequenced library, we observed a broad size distribution ranging from 35-bp to 333-bp (Fig. 2a). The input distribution was characterized by a sharp maximum at 147-bp, as expected for fully protected mononucleosomal DNA flanked by exposed DNA that is subject to endonucleolytic nicking, double-strand cleavage and end-nibbling, which is characteristic of single-strand-specific nucleases such as MNase26. In addition, maxima were observed at approximately 55, 90, and 130 bp, with a trail of longer fragments greater than 180 bp.

Similar distributions were seen for the affinity purified fractions, except that the 147-bp maxima were less prominent, and maxima also appeared around 170 bp. Because the large majority of fragments were mononucleosome or smaller in size, and no single fragment of the ~30 million sequenced was larger than 333 bp, we can be confident that our nucleosome purifications are not contaminated by tagged histones on neighboring nucleosomes.

Based on the distribution of fragment sizes and peaks, we binned the fragments into six size class intervals: 55, 90, 130, 147, 170, and >180-bp (Fig 2a, top). For each class, we divided all 10,997 genes for which both 5′ and 3′ ends are known into five quintiles based on expression levels and profiled the reads at the ends of the genes. A surprising finding was that input nucleosomal fragments in the 55-bp size class (35–75 bp interval) peaked ~20-bp upstream of the TSSs for genes in the first, second and third quintiles, which represent the transcriptionally active genes. This interval roughly corresponds to the average footprint of Pol II[27,28]. However, at least some of the peak may be nucleosomal, because fragments in this size class were also enriched after H2Av affinity purification. It is likely that any nucleosomes yielding such short DNA fragments are sufficiently disrupted for MNase to cleave extensively within the particle.

For all five size classes larger than 55 bp, a striking difference between heterotypic and homotypic H2Av nucleosomes was evident. Homotypic H2Av was strongly enriched immediately downstream of the TSS of actively transcribed genes, where heterotypic H2Av was relatively depleted (Fig. 2b and Supplementary Figs. 4–5). Peaks of homotypic H2Av nucleosomes displayed phasing from +1 to +4 with gradual dampening. The first homotypic H2Av expression quintile showed depletion compared to the second and third, which were similarly enriched. The fact that all five larger homotypic H2Av size classes independently showed the same profile, with only minor differences in peak resolution between quintiles, implies that these differences are robust. Furthermore, all five homotypic H2Av classes were strongly enriched compared to heterotypic H2Av. As a control we also sequenced the input fractions and, as expected, observed intermediate enrichments for the five larger size classes (Fig. 2b and Supplementary Fig. 4). We have previously shown that H2A-containing nucleosomes are strongly depleted downstream of TSSs in a pattern that is approximately inverse to that of H2Av[29], which, when taken together with the global abundance of H2Av[30], implies that homotypic H2Av nucleosomes predominate over the first few nucleosomes downstream of the TSS of active genes (Supplementary Fig. 6).

Homotypic H2Av nucleosomes are enriched at 5′ splice sites

We wondered whether 5′-to-3′ polar enrichment of homotypic H2Av nucleosomes is specific to TSSs, or instead represents a general property of nucleosomes undergoing disruption during active transcription. To distinguish between these possibilities, we asked whether similar 5′-to-3′ polarity occurs within gene bodies. When we profiled all 67,630 annotated intron/exon junctions we found that homotypic and total H2Av nucleosomes were enriched relative to heterotypic H2Av over the first nucleosome downstream of the 5′ intron/exon junction of active genes, decreasing in enrichment within exons for homotypic H2Av (Fig. 3a–b and Supplementary Fig. 7a–c). Furthermore, the first quintile displayed reduced enrichment for homotypic but not for heterotypic H2Av or for total (input) nucleosomes

(Supplementary Fig. 7a–c). The enrichment of heterotypic H2Av over exons is most likely accounted for by the higher G+C content of exons relative to introns (Supplementary Fig. 7d), and previous work has shown that exons have a higher nucleosome density31–33. However, the differences between homotypic and heterotypic H2Av must be independent of G+C content, because all five expression quintiles display identical average G+C content over introns and exons, whereas homotypic H2Av displays 5′-to-3′ polarity for the first three quintiles relative to the lowest two quintiles. We conclude that the enrichment features of homotypic H2Av nucleosomes are not specific for the boundary between TSSs and gene bodies, but rather are general consequences of encounters between the transcriptional elongation apparatus and regions of high nucleosome density.

Homotypic H2Av nucleosomes are low-salt-soluble

We previously used tiling microarray analysis to show that the distribution of H2Av around TSSs resembles that of low-salt-soluble nucleosomes29, where low-salt solubility defines classical ‘active’ chromatin34. We wondered whether this correspondence reflects an inherent property of homotypic H2Av nucleosomes, in which case one might suppose that the different structural properties of H2A.Z versus H2A within the nucleosome core contribute to the generation of active chromatin. To directly compare homotypic H2Av with active chromatin profiles, we prepared low-salt-soluble nucleosomes from S2 cells by extraction of intact MNased nuclei with 80mM NaCl and sequenced a library of fragments using the Illumina platform. As previously observed using tiling microarrays, the salt-solubility profile is all-or-none with respect to gene expression, in that the top three quintiles display profiles with peaks of similar height, whereas the lowest two quintiles, which represent inactive genes, display a featureless pattern (Fig. 3f). The +1 nucleosome downstream of the TSS is enriched in the 80mM soluble fraction, with strong phasing down to the +8 nucleosome and a gradual decay in amplitude. These features of classical active chromatin closely resemble those of both homotypic and total H2Av (Fig. 3d–e). We then investigated the peak spacing between low-salt-soluble nucleosomes and homotypic H2Av and found that they were virtually identical, both averaging ~175 bp (Supplementary Table 1). We also observed close correspondences between homotypic H2Av, total H2Av and low-salt-soluble nucleosomes downstream of intron/exon junctions, where successive peaks display similar 5′-to-3′ polarity (Fig. 3a–c). These results imply that the distinctive physical properties of active chromatin that cause it to be more easily solubilized by low salt arise, at least in part, from structural differences between homotypic H2Av and H2A-containing nucleosomes.

We have previously shown that low-salt-soluble nucleosomes are enriched at epigenetic regulatory elements, including those bound by the trithorax-Group protein, Zeste, and the Polycomb-Group proteins, Enhancer-of-Zeste (EZ) and Posterior-Sex-Combs (PSC). To ascertain whether a similar enrichment is seen for homotypic H2Av nucleosomes, we aligned sequenced fragments around protein binding sites and averaged over all sites. For the five larger size classes, no enrichment of H2Av of either type or input was seen over Zeste sites and little if any over EZ+PSC sites, although the 55-bp class was characterized by peaks for input, heterotypic, total, and homotypic H2Av nucleosomes (Supplementary Fig. 8). This pattern of enrichment at epigenetic regulatory elements is similar to the pattern

found at promoters of active genes, where only the 55-bp class is enriched over the TSS (Fig. 2b). At both epigenetic regulatory elements and TSSs, nucleosomes are relatively depleted, which implies that only particles that are unstable and relatively accessible to MNase are detected, whereas homotypic H2A.Z nucleosomes are especially stable21. Therefore, the enrichment of homotypic H2A.Z nucleosomes does not seem to be a general feature of classical active chromatin, but rather is specific for nucleosome-dense genic regions undergoing transcriptional elongation.

RNA Polymerase II pauses at H2Av depleted genes

Enrichment of homotypic H2Av nucleosomes where Pol II encounters more densely packed low-salt-soluble nucleosomes raised the question of whether the process of homotypic enrichment is related to the degree of polymerase transit. One situation in which polymerase transit differs between genes is at sites of pausing downstream of the TSS in various animal systems35–37. Release of RNA Pol II from the paused state is the rate-limiting step in transcription of these genes. Therefore, we asked whether the genes that are subject to pausing downstream of TSSs in S2 cells are more or less likely to be enriched in homotypic H2Av than are genes that are not subject to pausing. Using *Drosophila* S2 cell data from a study that identified 1014 stalled genes and 4392 active genes that were not stalled36, we observed a general depletion of nucleosomes over gene bodies in the stalled class relative to those in the unstalled class (Fig. 4a, bottom panel). We attribute this decrease to the lower G +C content of genes in the stalled class compared to genes in the unstalled class (Supplementary Fig. 7a). Relative to this difference, we see a striking enrichment of homotypic H2Av and equal depletion of heterotypic H2Av nucleosomes in the unstalled relative to the stalled class (Fig. 4a, top and middle panels). The lower level of homotypic H2Av in the stalled class relative to the unstalled class is not accounted for by lower overall expression of stalled genes, because this class shows a slight enrichment of expressed genes relative to the unstalled class (Supplementary Fig. 9a).

To better understand why homotypic H2Av is depleted from the stalled class, we examined the spacing between homotypic H2Av peaks downstream of the TSSs. It was previously reported that phased H2Av nucleosomes are shifted 10-bp downstream at paused genes compared to those that are not paused12. We likewise noted a downstream shift in our homotypic H2Av nucleosome peaks, in that increases in gene expression were correlated with increasing downstream shifts. At the +1 nucleosome, the first expression quintile displayed a 10-bp peak downstream from the second quintile, which displayed a 10-bp shift compared to the third (Fig. 4b). Similar shifts downstream of the TSS were seen for input nucleosomes (Supplementary Fig. 9b), likely reflecting the predominance of homotypic H2Av at these nucleosome positions. Peak shifts increased in length for the +2 and +3 nucleosomes, so that the peaks for the +3 nucleosome was centered 520 bp, 500 bp, and 470 bp downstream of the TSSs for the first, second and third expression quintiles, respectively. These increases in peak spacing with increasing transcription suggest that homotypic H2Av nucleosomes are displaced downstream during transcriptional elongation. However, no difference in peak shift was detected between nucleosomes in the stalled and unstalled classes (Fig. 4b and Supplementary Fig. 9b). Therefore, the propensity for a homotypic H2Av nucleosome to be displaced downstream during polymerase passage does not seem to

depend on whether or not the polymerase is stalled. Rather, this propensity might depend on some inherent property of homotypic H2A.Z nucleosomes.

Active chromatin is depleted from genes with paused RNA Pol II

One property of homotypic H2Av nucleosomes that might contribute to their depletion at paused genes is their low-salt solubility. Indeed, when we examined profiles of low-salt-soluble nucleosomes for stalled and unstalled genes, we detected a striking difference: The stalled gene profile displayed a pair of narrow low-salt-soluble peaks, at −20 bp and +80 bp relative to the TSS, with very low levels of low-salt-soluble nucleosomes downstream, whereas no such peaks were observed in unstalled genes (Fig. 5a, dotted blue lines). The 100-bp spacing of these peaks is less than the 150-bp spacing that we would expect for bona fide nucleosomes, which we had assumed in combining plus- and minus-strand reads to display the 80mM single-read data (Figs. 3a and 3d). Therefore, we asked whether these peaks instead represent protection by a particle located directly in between the two peaks, centered over +30 but only in genes with paused Pol II. To evaluate this possibility, we mapped the ends of the plus and minus reads without any offset to compensate for peak spacing. This revealed that their distributions approximately coincide around a peak centered over +30 (Fig. 5, top panels, green and orange lines), rather than showing further peak splitting as would be expect for phased nucleosomes. The coincidence of plus- and minus-strand reads without offset implies that they result from protection of DNA from MNase digestion by a very small particle that is located on average at +30.

To confirm that the protected particle is at the precise location of paused Pol II, we performed limited paired-end sequencing of low-salt-soluble chromatin. By mapping and binning reads in the 25–75 bp range, we detected a sharp peak ~50-bp wide centered over +30 for active genes in the stalled class, with a relatively small peak at this location for genes in the unstalled class (Fig. 5b, bottom panels). As +30 is the mean location of paused RNA Pol II36, we infer that our sequence mapping of classical active chromatin has accurately footprinted this species, which implies that paused Pol II is itself enriched in low-salt-soluble chromatin29.

We also observed that phased low-salt-soluble nucleosomes downstream of paused Pol II were strongly depleted relative to those in the unstalled class (Fig. 5b). This implies that pausing inhibits the generation of low-salt-soluble active chromatin downstream. Therefore, genes with paused Pol II are deficient for both homotypic H2Av nucleosomes and low-salt-soluble nucleosomes, which provides additional evidence that homotypic H2A.Z is a key attribute of transcriptionally active chromatin.

DISCUSSION

Our mapping of individual H2Av nucleosomes across the *Drosophila* genome has revealed unexpected differences between homotypic and heterotypic H2A.Z nucleosomes. First, only homotypic H2A.Z nucleosomes are enriched over genes, whereas heterotypic nucleosomes are depleted. Second, a physical property of chromatin, namely its solubility, co-localizes with the distribution of homotypic H2A.Z. Third, both homotypic H2A.Z and low-salt solubility of nucleosomes correspond to one another at intron/exon junctions in the same

manner as at transcriptional start sites, which implies that properties of homotypic H2A.Z nucleosomes result from RNA Polymerase II transit. Fourth, genes with paused Pol II are depleted in both homotypic H2A.Z and low-salt-soluble nucleosomes, further suggesting that homotypic H2A.Z nucleosomes and classical active chromatin are generated during transcriptional elongation. These findings have implications both for understanding the mechanism whereby H2A.Z becomes preferentially enriched at active genes and for how H2A.Z might function in transcriptional regulation.

Homotypic H2A.Z nucleosomes differ structurally from canonical H2A nucleosomes16, and we suggest that these differences in localization and *in vivo* properties result from an underlying structural difference between nucleosomes of different composition. An obvious candidate for such a structural difference is the interface between H2A/H2B dimers within the nucleosome core22,38. This dimerization interface is more extensive for H2A.Z/H2A.Z than for H2A/H2A, and there is a potential structural clash between H2A.Z and H2A in the same core particle16. However, heterotypic H2A.Z nucleosomes form readily *in vitro*17 and are abundant *in vivo*18, and we have found that they are broadly distributed genome-wide. Alternatively, the conserved differences in the docking domains of H2A.Z and H2A might be responsible for their differences in distribution and *in vivo* properties. In either case, heterotypic H2Av nucleosomes might be sufficiently stable to assemble, but more likely than homotypic H2Av nucleosomes to unravel when disrupted. Nucleosomes are disrupted over promoters of active genes, where unstable core particles containing both H3.3 and H2A.Z from human cells have been found to be enriched39. It is possible that these unstable double-variant nucleosomes are more accessible to internal cleavage by MNase, and so might correspond to the 55-bp class of TSS-derived small DNA fragments that we obtained from H2Av-containing nucleosomes (Fig. 2b, bottom panels).

The enrichment of H2A.Z downstream of TSSs and intron/exon junctions might be understood by a simple model based on relative stability of homotypic H2A.Z nucleosomes to disruption by RNA Pol II transit, and the *in vitro* observation that RNA Pol II evicts an H2A/H2B dimer when it transcribes through a nucleosome40 (Fig. 6). When a dimer is occasionally lost at random *in vivo*, the resulting hexameric particle becomes a substrate for new dimer addition, which can be either H2A-H2B or H2A.Z-H2B. If replacement is by the Swr1 complex then an H2A.Z-H2B dimer will be deposited11, forming a heterotypic nucleosome. A subsequent round of transcriptional elongation would lead to occasional loss of either dimer. When the loss is of the remaining H2A-H2B followed by the gain of a second H2A.Z-H2B, a homotypic H2A.Z nucleosome will result. One possibility is that the more extensive dimerization interface between the two H2A.Zs in the core particle16 would make them more stable than either canonical H2A/H2A or heterotypic H2A.Z/H2A to unraveling and losing a dimer by subsequent Pol II encounters. Alternatively, the docking domain of H2A.Z might interact more stably with the $(H3/H4)_2$ tetramer and thus show a lower propensity to be lost than H2A. Thus, the more rounds of transcription through a nucleosome position, the more likely it will be that a nucleosome will be homotypic for H2A.Z and the more likely that it will be extracted by low-salt because it is repeatedly disrupted. In this way the unique intranucleosomal interaction between H2A variants would ultimately be responsible for altering the physical properties of chromatin.

Our observation that homotypic H2A.Z nucleosomes are depleted over genes with stalled polymerases argues against proposals that H2A.Z nucleosomes act as simple barriers to transcriptional elongation12,22. Rather, our results suggest that homotypic H2A.Z nucleosomes facilitate, not impede, transcriptional elongation. They might do this, for example, by recruiting ATP-dependent nucleosome remodelers, such as ISWI, which preferentially mobilizes H2A.Z nucleosomes41. We speculate that when homotypic H2A.Z nucleosomes are mobilized, they facilitate polymerase transit by helping to relieve torsional strain. RNA polymerase creates positive torsion ahead and negative torsion behind as it moves a denatured DNA bubble forward. When it approaches a nucleosome, the positive torsional stress helps to unravel the left-handed nucleosome core particle42. At the same time, the negative torsional stress in the wake of polymerase helps to rewind the DNA around the nucleosome core. A wave of positive torsional stress ahead of and negative torsional stress behind elongating RNA Pol II is thought to facilitate nucleosome disassembly and reassembly43–45. We propose that the distinct interaction surfaces of H2A.Z facilitate nucleosome reformation in the wake of elongating polymerases, thus more rapidly taking up negative supercoils and relieving the negative strain caused by polymerase transit. Relief of negative strain is expected to reduce backtracking of RNA Polymerase II, which is thought to be the mechanistic basis for polymerase stalling46. Thus, enrichment of homotypic H2A.Z nucleosomes at TSSs would be a general adaptation for relieving paused polymerase at TSSs and downstream.

The enrichment of Drosophila H2Av over phased nucleosomes is typical for H2A.Z patterns seen in plants, fungi and other animals13–15,47. However, *Drosophila* is unique in that its H2A.Z has acquired a functional C-terminal SQ(E/D)Φ motif (where Φ represents a hydrophobic residue), which in other eukaryotes is present on H2A.X, a replication-independent variant that belongs to the H2A clade1. The function of the SQ(E/D)Φ motif is well-established: SQ(E/D)Φ serines in the vicinity of a double-strand (ds) break become rapidly phosphorylated, and the resulting γ–H2AX phosphates help to recruit the homologous ds DNA repair machinery to facilitate accurate repair48. Because ds breaks can occur anywhere, H2A.X must be ubiquitously distributed throughout the genome. Nucleosome disruption during replication fork passage might result in such a ubiquitous H2Av distribution genome-wide. Thus, the uniformity of heterotypic H2Av throughout the genome might be seen as a feature that has allowed *Drosophila* to dispense with its ancestral H2A.X after acquisition of the SQ(E/D)Φ motif at the C-terminus of its only other replication-independent H2A variant. Our results imply that only homotypic H2Av participates in transcriptional regulation, whereas the relative uniformity of heterotypic H2Av may have permitted the acquisition of a ubiquitous DNA repair function. Thus, the distinct structural features of heterotypic and homotypic H2Av might have led to the evolution of H2Av bifunctionality.

METHODS

Cell Culture and Transgene Expression

Stable *Drosophila* S2 cell lines were created as described50,51. We expressed FLAG-tagged H2Av in these lines with baculovirus under the metallothionein promoter as described52.

Briefly, we infected one 150 cm^2 flask of 6×10^7 BLRP-H2A and BLRP-H2Av cells and one flask of S2 cells with a baculovirus construct encoding FLAG-H2Av for two hours at a multiplicity of infection of 100. We then added fresh media and induced transgene expression with 0.5 mM $CuS0_4$ for 72 hours.

Chromatin Preparation

We prepared chromatin for affinity purification essentially as described52, except that we fixed soluble nucleosomes with formaldehyde prior to affinity purification. Briefly, ~3×10^8 cells from each flask were suspended in HM2 (10 mM Hepes, 2 mM $MgCl_2$, 0.5 mM phenylmethanesulphonylfluoride (PMSF)) and lysed with 0.6% (v/v) NP-40. Nuclei were resuspended in 900 μl HM2 and $CaCl_2$ was added to ~1 mM, and warmed to 37° for 2′. We digested chromatin with 1 U of MNase for 10′, and stopped the reaction by adding 5 mM EDTA and incubated for 30′ on ice. We checked for nuclear retention of total chromatin on protein gels, and detected only ~1.5% of the total released into the soluble fraction (Supplementary Fig. 11). Nuclei were resuspended in HE buffer (10 mM Hepes 0.25 mM EDTA 0.5 mM PMSF) and chromatin was needle-extracted25. Soluble chromatin following MNase and needle extraction was diluted to an OD_{260} of 3–3.5 (10 mm path) with HE, fixed for 1 hr at RT with 1% (w/v) fresh formaldehyde (pH 7.0), quenched with 125 mM glycine, and dialyzed for 1hour with three changes of HE buffer at 4°. Overall recovery of MNased nucleosomes averaged ~60%. We removed 150 μl to serve as input chromatin and used the remainder for affinity purification. We found that tagged H2Av nucleosomes included the same approximate ratio of tagged and untagged H2A as input chromatin (Supplementary Fig. 1c).

We prepared 80 mM soluble chromatin as described29. We found that profiling of H2Av-containing nucleosomes from this material led to highly inconsistent results (S.H., unpublished results), perhaps owing to the reported instability of double-variant H3.3+H2A.Z nucleosomes when subjected to such salt treatments39.

Chromatin affinity purification

We incubated chromatin with 50 μl of equilibrated Anti-FLAG affinity agarose beads (Sigma, A2222) overnight at 4°C with end-over-end rotation. Beads were collected by centrifugation, the unbound fraction was collected, and the beads were washed with HE supplemented with 150 mM NaCl and 0.1% Triton X-100 (v/v), 3x and then 2x with HE buffer, 10′ on a rotator for each wash to yield single-FLAG-H2Av pulldown material (total H2Av). For sequential affinity purification we eluted the bound FLAG-H2Av nucleosomes with 200 μl of 100 μg ml^{-1} 3xFLAG peptide in HE, 30′ at 4°, the supernatant was collected, and the elution was repeated 2 × 10′ at RT. The beads were then washed with 400 μl HE and the supernatant was added to eluate. We then centrifuged the entire eluate 5′ at 2,200×*g*, and the supernatant was incubated with 50 μl packed streptavidin-sepharose (GE) for 3 hr on a rotator at 4°C and washed as before.

Illumina library construction and sequencing

Affinity purified nucleosomes from a single FLAG-H2Av (total H2Av) and two biological replicates for input, heterotypic, and homotypic purification were incubated with 0.1M NaCl

and 10 mM EDTA for 4 hours at 65° to reverse the formaldehyde crosslinks. DNA was purified as described29, except that the Proteinase K digestion was extended to 1 hour. We prepared libraries with 100 ng of DNA as described (Illumina) and size-selected our libraries after linker addition to a total length of 100–600 bp. Samples were sequenced in paired-end mode (36-bp read length). For the 80 mM soluble chromatin we prepared libraries from 500 ng of DNA as described (Illumina) and size-selected our libraries to 100–600 bp. This library was sequenced in single-end mode (35-bp read length).

Data Processing

For paired-end data we aligned uniquely mapped 35-bp reads with paired-end alignment score greater than zero to Release 5 of the *Drosophila melanogaster* reference sequence (http://flybase.org) using Eland (Illumina) or Novoalign (Novocraft). Each interval count was divided by the total number of counts and rescaled by multiplying by 10^9.

To analyze reads by length, we divided up paired-end fragments into the following size classes: 55-bp (35–75 bp), 90-bp (76–110 bp), 130-bp (111–140 bp), 147-bp (141–160 bp), 170-bp (161–180 bp), > 180-bp (181–333 bp) and repeated the above processing for each size class, normalizing to the total number of counts for the size class.

For single-end data, we used all uniquely mapped reads and selected one location at random for reads that mapped to more than one location on the genome. We moved the position of each read to the middle of a 150-bp fragment, fit a Gaussian kernel density function with bandwidth 20 bp at 10-bp intervals, and normalized so that the values for each 10-bp interval equaled the number of reads for the chromosome arm. For individual strand analysis, we used only the reads mapped to the plus or minus strand and did not re-locate the read position before fitting the kernel density function53.

Data Analysis

To analyze gene ends, we used 10,997 euchromatic genes with both the 5′ and 3′ ends annotated in FlyBase r5.23. If a gene had more than one transcript we used the longest one. We then rank-ordered genes based on expression level in S2 cells29, split these genes into quintiles, and calculated the average number of normalized reads using 10-bp bins. Contributions from neighboring transcription units were omitted during averaging. For stalled and unstalled genes we matched 950 stalled and 4,061 unstalled genes36. We repeated the ends analysis but filtered the gene to these two sets. We used 67,630 unique exons in euchromatin annotated in FlyBase r5.23. Transposons were analyzed essentially as previously described29. For analysis of epigenetic regulatory elements, we used published Zeste54 and EZ-PSC55 ChIP-chip binding data as previously described29, and averaged the paired-end data for all size classes at 50-bp resolution.

Supplementary Material

Refer to Web version on PubMed Central for supplementary material.

Acknowledgments

We thank Friedemann Loos for participating in early stages of this study, Andy Marty of the Hutchinson Center Shared Genomics Resource for Illumina sequencing, Elizabeth Greene for help with Solexa analysis, Robert Glaser (Wadsworth Center, New York State Department of Health) for the H2Av antibody and Melissa Conerly, Roger Deal, Paul Talbert and Erika Wolff for critical comments. This work was supported by the Howard Hughes Medical Institute.

References

1. Talbert PB, Henikoff S. Histone variants--ancient wrap artists of the epigenome. Nat Rev Mol Cell Biol. 2010; 11:264–75. [PubMed: 20197778]
2. Palmer D, Snyder LA, Blumenfeld M. Drosophila nucleosomes contain an unusual histone-like protein. Proceedings of the National Academy of Sciences of the United States of America. 1980; 77:2671–75. [PubMed: 6771757]
3. Wu RS, Tsai S, Bonner WM. Patterns of histone variant synthesis can distinguish G0 from G1 cells. Cell. 1982; 31:367–74. [PubMed: 7159927]
4. Zlatanova J, Thakar A. H2A.Z: view from the top. Structure. 2008; 16:166–79. [PubMed: 18275809]
5. Liu X, Li B, Gorovsky M. Essential and nonessential histone H2A variants in Tetrahymena thermophila. Mol Cell Biol. 1996; 16:4305–11. [PubMed: 8754831]
6. Ridgway P, Brown KD, Rangasamy D, Svensson U, Tremethick DJ. Unique residues on the H2A.Z containing nucleosome surface are important for Xenopus laevis development. J Biol Chem. 2004; 279:43815–20. [PubMed: 15299007]
7. Faast R, et al. Histone variant H2A.Z is required for early mammalian development. Current Biology. 2001; 11:1183–7. [PubMed: 11516949]
8. van Daal A, Elgin SC. A histone variant, H2AvD, is essential in Drosophila melanogaster. Molecular Biology of the Cell. 1992; 3:593–602. [PubMed: 1498368]
9. Kobor MS, et al. A Protein Complex Containing the Conserved Swi2/Snf2-Related ATPase Swr1p Deposits Histone Variant H2A.Z into Euchromatin. PLoS Biology. 2004; 2:E131. [PubMed: 15045029]
10. Krogan NJ, et al. A Snf2 family ATPase complex required for recruitment of the histone H2A variant Htz1. Molecular Cell. 2003; 12:1565–1576. [PubMed: 14690608]
11. Mizuguchi G, Shen X, Landry J, Wu WH, Sen S, Wu C. ATP-driven exchange of histone H2AZ variant catalyzed by SWR1 chromatin remodeling complex. Science. 2004; 303:343–348. [PubMed: 14645854]
12. Mavrich TN, et al. Nucleosome organization in the Drosophila genome. Nature. 2008
13. Barski A, et al. High-resolution profiling of histone methylations in the human genome. Cell. 2007; 129:823–37. [PubMed: 17512414]
14. Zilberman D, Coleman-Derr D, Ballinger T, Henikoff S. Histone H2A.Z and DNA methylation are mutually antagonistic chromatin marks. Nature. 2008; 456:125–129. [PubMed: 18815594]
15. Lantermann AB, Straub T, Stralfors A, Yuan GC, Ekwall K, Korber P. Schizosaccharomyces pombe genome-wide nucleosome mapping reveals positioning mechanisms distinct from those of Saccharomyces cerevisiae. Nat Struct Mol Biol. 2010; 17:251–7. [PubMed: 20118936]
16. Suto RK, Clarkson MJ, Tremethick DJ, Luger K. Crystal structure of a nucleosome core particle containing the variant histone H2A.Z. Nature Structural Biology. 2000; 7:1121–1124. [PubMed: 11101893]
17. Chakravarthy S, Bao Y, Roberts VA, Tremethick D, Luger K. Structural characterization of histone H2A variants. Cold Spring Harb Symp Quant Biol. 2004; 69:227–34. [PubMed: 16117653]
18. Viens A, Mechold U, Brouillard F, Gilbert C, Leclerc P, Ogryzko V. Analysis of human histone H2AZ deposition in vivo argues against its direct role in epigenetic templating mechanisms. Molecular and Cellular Biology. 2006; 26:5325–35. [PubMed: 16809769]

19. Park YJ, Dyer PN, Tremethick DJ, Luger K. A new fluorescence resonance energy transfer approach demonstrates that the histone variant H2AZ stabilizes the histone octamer within the nucleosome. Journal of Biological Chemistry. 2004; 279:24274–82. [PubMed: 15020582]
20. Li W, Nagaraja S, Delcuve GP, Hendzel MJ, Davie JR. Effects of histone acetylation, ubiquitination and variants on nucleosome stability. Biochemical Journal. 1993; 296 (Pt 3):737–44. [PubMed: 8280071]
21. Thambirajah AA, Dryhurst D, Ishibashi T, Li A, Maffey AH, Ausio J. H2A.Z stabilizes chromatin in a way that is dependent on core histone acetylation. Journal of Biological Chemistry. 2006; 281:20036–44. [PubMed: 16707487]
22. Thakar A, Gupta P, McAllister WT, Zlatanova J. Histone variant H2A.Z inhibits transcription in reconstituted nucleosomes. Biochemistry. 2010
23. Ishibashi T, Dryhurst D, Rose KL, Shabanowitz J, Hunt DF, Ausio J. Acetylation of Vertebrate H2A.Z and Its Effect on the Structure of the Nucleosome. Biochemistry. 2009; 48:5007–5017. [PubMed: 19385636]
24. Malik HS, Henikoff S. Phylogenomics of the nucleosome. Nat Struct Biol. 2003; 10:882–891. [PubMed: 14583738]
25. Jin C, Felsenfeld G. Nucleosome stability mediated by histone variants H3.3 and H2A.Z. Genes and Development. 2007; 21:1519–29. [PubMed: 17575053]
26. Desai NA, Shankar V. Single-strand-specific nucleases. FEMS Microbiology Reviews. 2003; 26:457–491. [PubMed: 12586391]
27. Buratowski S, Hahn S, Guarente L, Sharp PA. Five intermediate complexes in transcription initiation by RNA polymerase II. Cell. 1989; 56:549–61. [PubMed: 2917366]
28. Selby CP, Drapkin R, Reinberg D, Sancar A. RNA polymerase II stalled at a thymine dimer: Footprint and effect on excision repair. Nucleic Acids Research. 1997; 25:787–793. [PubMed: 9016630]
29. Henikoff S, Henikoff JG, Sakai A, Loeb GB, Ahmad K. Genome-wide profiling of salt fractions maps physical properties of chromatin. Genome Research. 2009; 19:460–9. [PubMed: 19088306]
30. Palmer D, Snyder LA, Blumenfeld M. Drosophila nucleosomes contain an unusual histone-like protein. Proc Natl Acad Sci U S A. 1980; 77:2671–75. [PubMed: 6771757]
31. Schwartz S, Meshorer E, Ast G. Chromatin organization marks exon-intron structure. Nature Structural & Molecular Biology. 2009; 16:990–U117.
32. Sims RJ, et al. Recognition of trimethylated histone h3 lysine 4 facilitates the recruitment of transcription postinitiation factors and pre-mRNA splicing. Molecular Cell. 2007; 28:665–676. [PubMed: 18042460]
33. Tilgner H, et al. Nucleosome positioning as a determinant of exon recognition. Nat Struct Mol Biol. 2009; 16:996–1001. [PubMed: 19684599]
34. Rocha E, Davie JR, van Holde KE, Weintraub H. Differential salt fractionation of active and inactive genomic domains in chicken erythrocyte. Journal of Biological Chemistry. 1984; 259:8558–63. [PubMed: 6736042]
35. Rougvie AE, Lis JT. Postinitiation transcriptional control in Drosophila melanogaster. Molecular Cell. 1990; 10:6041–6045.
36. Muse GW, et al. RNA polymerase is poised for activation across the genome. Nature Genetics. 2007; 39:1507–11. [PubMed: 17994021]
37. Rahl PB, et al. c-Myc regulates transcriptional pause release. Cell. 2010; 141:432–45. [PubMed: 20434984]
38. Henikoff S. Labile H3.3+H2A.Z nucleosomes mark ‘nucleosome-free regions’. Nat Genet. 2009; 41:865–6. [PubMed: 19639024]
39. Jin C, et al. H3.3/H2A.Z double variant-containing nucleosomes mark ‘nucleosome-free regions’ of active promoters and other regulatory regions in the human genome. Nature Genetics. 2009; 41:941–45. [PubMed: 19633671]
40. Kireeva ML, Walter W, Tchernajenko V, Bondarenko VA, Kashley M, Studitsky VM. Nucleosome remodeling induced by RNA polymerase II: loss of the H2A/H2B dimer during transcription. Molecular Cell. 2002; 9:541–552. [PubMed: 11931762]

41. Goldman JA, Garlick JD, Kingston RE. Chromatin remodeling by imitation switch (ISWI) class ATP-dependent remodelers is stimulated by histone variant H2A.Z. J Biol Chem. 2010; 285:4645–51. [PubMed: 19940112]
42. van Holde KE, Lohr DE, Robert C. What happens to nucleosomes during transcription? Journal of Biological Chemistry. 1992; 267:2837–2840. [PubMed: 1310672]
43. Kouzine F, Sanford S, Elisha-Feil Z, Levens D. The functional response of upstream DNA to dynamic supercoiling in vivo. Nat Struct Mol Biol. 2008; 15:146–54. [PubMed: 18193062]
44. Bancaud A, et al. Nucleosome chiral transition under positive torsional stress in single chromatin fibers. Mol Cell. 2007; 27:135–47. [PubMed: 17612496]
45. Wang Z, Droge P. Differential control of transcription-induced and overall DNA supercoiling by eukaryotic topoisomerases in vitro. Embo J. 1996; 15:581–9. [PubMed: 8599941]
46. Galburt EA, et al. Backtracking determines the force sensitivity of RNAP II in a factor-dependent manner. Nature. 2007; 446:820–3. [PubMed: 17361130]
47. Albert I, et al. Translational and rotational settings of H2A.Z nucleosomes across the Saccharomyces cerevisiae genome. Nature. 2007; 446:572–6. [PubMed: 17392789]
48. Fernandez-Capetillo O, Lee A, Nussenzweig M, Nussenzweig A. H2AX: the histone guardian of the genome. DNA Repair (Amst). 2004; 3:959–67. [PubMed: 15279782]
49. Madigan JP, Chotkowski HL, Glaser RL. DNA double-strand break-induced phosphorylation of Drosophila histone variant H2Av helps prevent radiation-induced apoptosis. Nucleic Acids Res. 2002; 30:3698–705. [PubMed: 12202754]
50. Mito Y, Henikoff JG, Henikoff S. Genome-scale profiling of histone H3.3 replacement patterns. Nat Genet. 2005; 37:1090–7. [PubMed: 16155569]
51. Henikoff S, Henikoff JG, Sakai A, Loeb GB, Ahmad K. Genome-wide profiling of salt fractions maps physical properties of chromatin. Genome Res. 2009; 19:460–9. [PubMed: 19088306]
52. Bryson TD, Weber CM, Henikoff S. Baculovirus-encoded protein expression for epigenomic profiling in Drosophila cells. Fly. 2010 In press.
53. Gehring M, Bubb K, Henikoff S. Extensive demethylation of repetitive elements during seed development underlies gene imprinting. Science. 2009; 324:1447–51. [PubMed: 19520961]
54. Moses AM, et al. Large-Scale Turnover of Functional Transcription Factor Binding Sites in Drosophila. PLoS Comput Biol. 2006; 2:e130. [PubMed: 17040121]
55. Schwartz YB, et al. Genome-wide analysis of Polycomb targets in Drosophila melanogaster. Nat Genet. 2006; 38:700–5. [PubMed: 16732288]

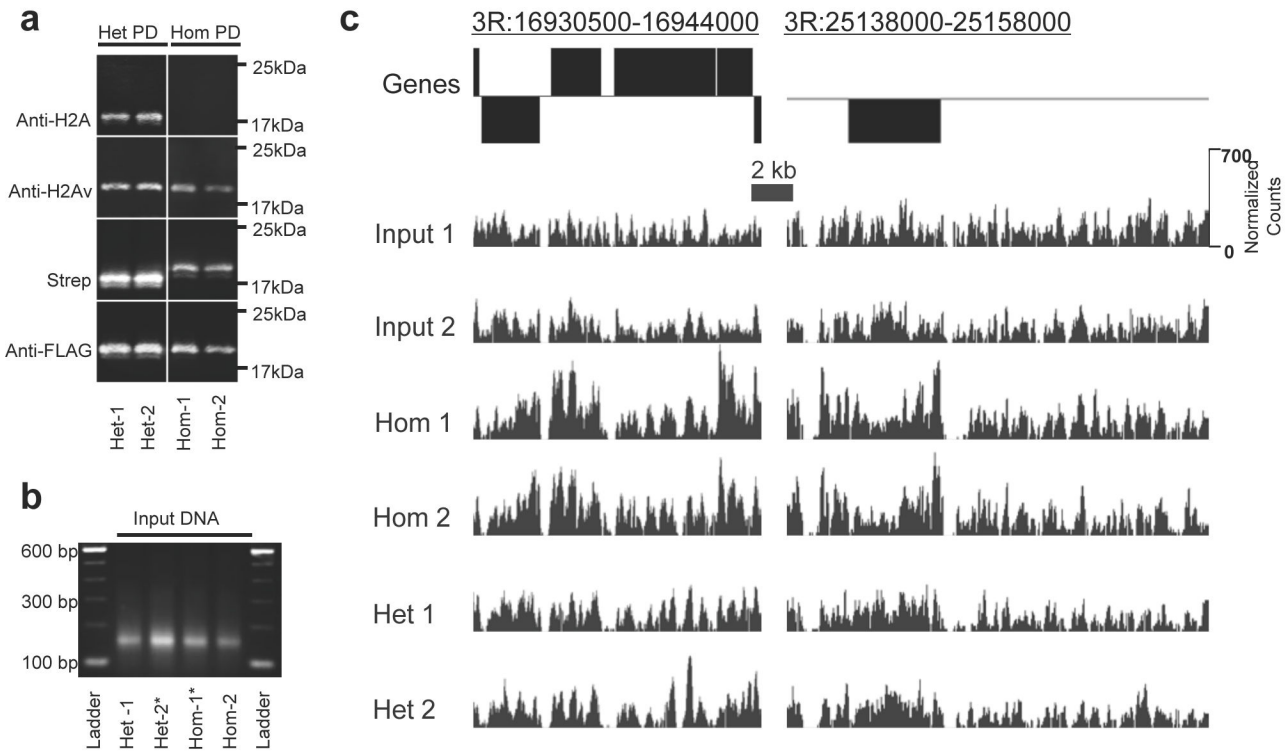

Figure 1.

Broad distribution of homotypic and heterotypic H2Av nucleosomes. (**a**) Western analyses of two replicates shows that sequential affinity-purified heterotypic and homotypic nucleosomes contain the expected composition of tagged histones and that endogenous epitopes are preserved. From the heterotypic purification (Het PD), antibodies (or streptavidin) recognize endogenous epitopes and tags from Biotag-H2A (16.9kDa) and FLAG-H2Av (18kDa). From the homotypic purification (Hom PD), antibodies [anti-H2A (Upstate 07-146), anti-H2Av49 or anti-FLAG (Sigma, F3165)] or streptavidin recognize endogenous epitopes and tags from Biotag-H2Av (18.5kDa) and FLAG-H2Av (H2Av). Proteins extracted from streptavidin beads with affinity-purified nucleosomes were resolved on 18% (w/v) SDS-PAGE gels and transferred to nitrocellulose. (**b**) Agarose gel showing that input DNA (1μg) comprises mostly mononucleosomal fragments for two replicates. Asterisks mark input samples that were sequenced. (**c**) Normalized counts in 10-bp intervals from representative regions of chromosome 3R, showing two biological replicates for all DNA sizes for input, homotypic, and heterotypic sequenced libraries.

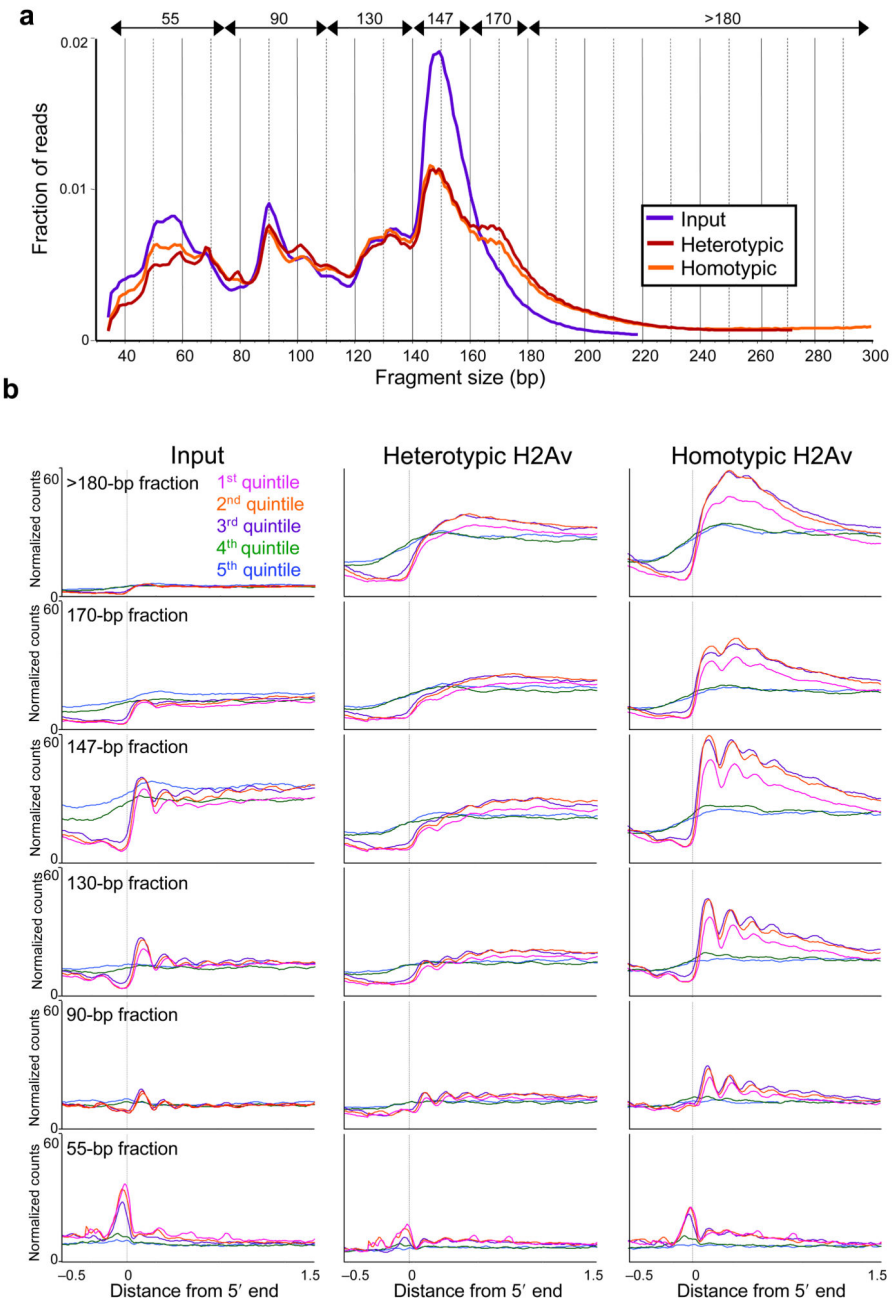

Figure 2.

Homotypic H2Av nucleosomes are enriched downstream of gene promoters. (**a**) Histogram showing the length distribution of mapped paired-end reads from the mean of two biological replicates for input, heterotypic, and homotypic H2Av purifications. The size range of binned reads is indicated at the top of the graph by arrows and the corresponding size class is labeled. (**b**) Average profiles for input, heterotypic, and homotypic H2Av purifications for the six size-class intervals: 55-bp (35–75bp), 90-bp (76–110bp), 130-bp (111–140bp), 147-bp (141–160bp), 170-bp (161–180bp), >180-bp (181–333bp). Genes were divided into quintiles based on expression level for all 10,997 fully annotated genes, aligned at their

TSSs and averaged within 10-bp bins. Averaging was truncated at 5′ or 3′ ends of neighboring genes. The *y*-axis refers to mapped paired-end counts. See also Supplementary Fig. 4 for 3′ ends as well.

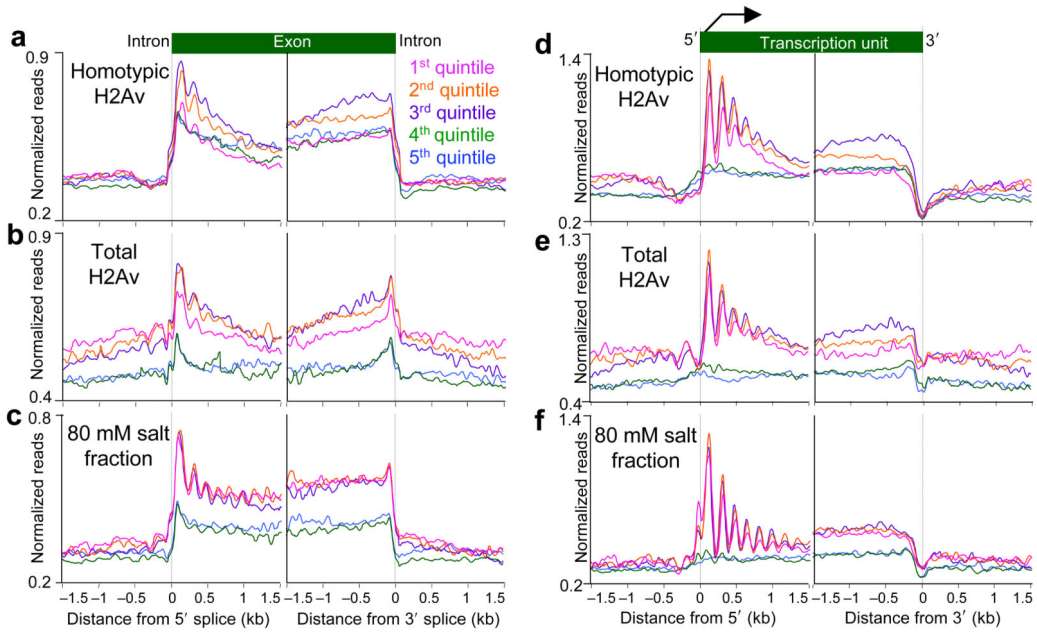

Figure 3.

Homotypic H2Av nucleosomes are enriched downstream of intron/exon Junctions and are low-salt-soluble. (**a)** Average profile for homotypic H2Av nucleosomes within the 147-bp size class aligned at intron/exon and exon/intron junctions and split into quintiles of gene expression as in Figure 2. (**b**) Single FLAG-H2Av pulldown (total H2Av) profile for comparison to **a**. (**c**) Average profile for DNA from 80mM soluble nucleosomes. Profiles in (**a–c**) represent means of biological replicates over 67,630 intron/exon junctions, divided into 10-bp bins. (**d–f**) Same as (**a–c)** except aligned around gene 5′ and 3′ ends. The *y*-axis refers to mapped single-end reads, where the scales were adjusted slightly to facilitate peak comparisons between the panels.

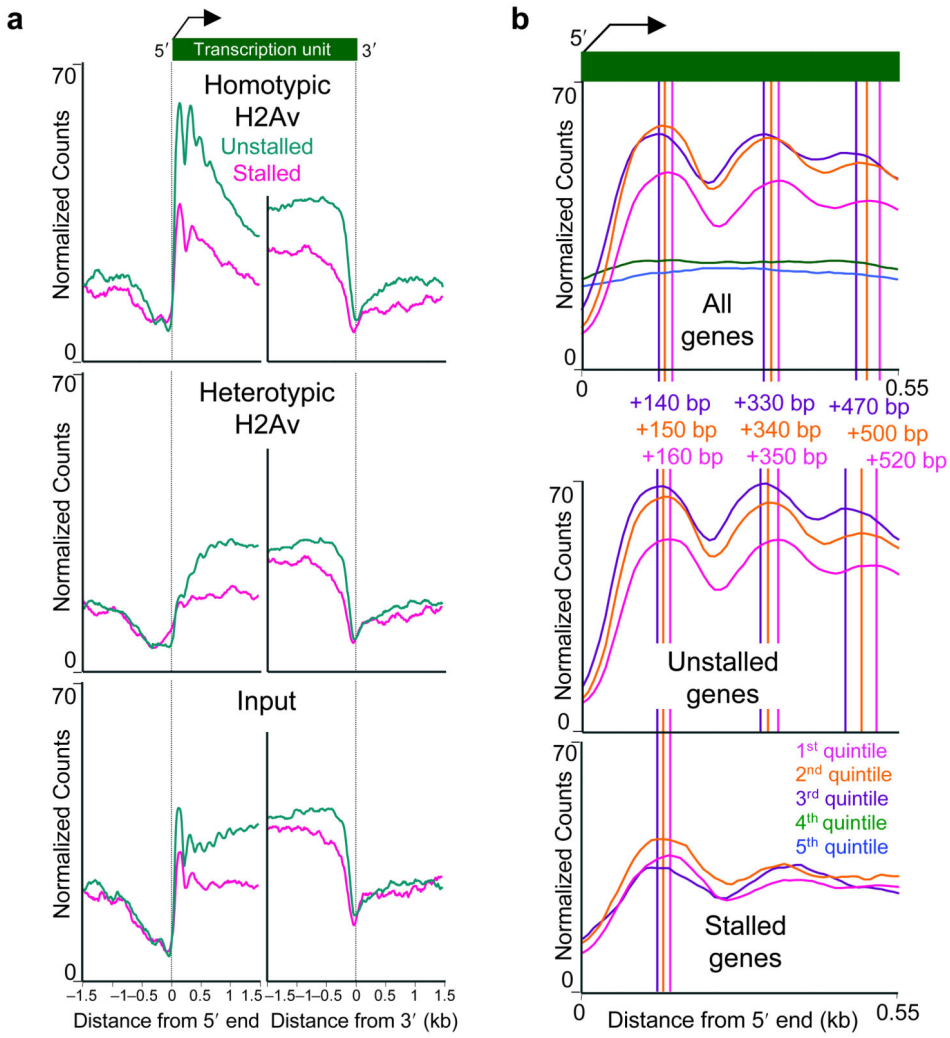

Figure 4.

Depletion of homotypic H2Av nucleosomes at genes with stalled RNA Polymerase II. (**a**) Average profiles for homotypic and heterotypic H2Av and input nucleosomes within the 147-bp size class for 950 genes that have promoter-proximal enrichment of polymerase (stalled, red) and 4061 genes that have polymerase throughout the genes but are not enriched proximal to the promoter (green). (**b**) Genes with and without stalled Pol II show displacement of homotypic H2Av nucleosomes with increasing expression level. Average profiles for homotypic H2Av nucleosomes within the 147-bp size class show shifting of peaks downstream with increasing expression for the top three quintiles, and relative depletion of the top expression quintile. Similar results are seen for the 950 stalled and the 4061 unstalled genes. Only the +1 position is shown for stalled genes because there are fewer genes and the resolution is lower than for unstalled genes. The *y*-axis refers to paired-end counts.

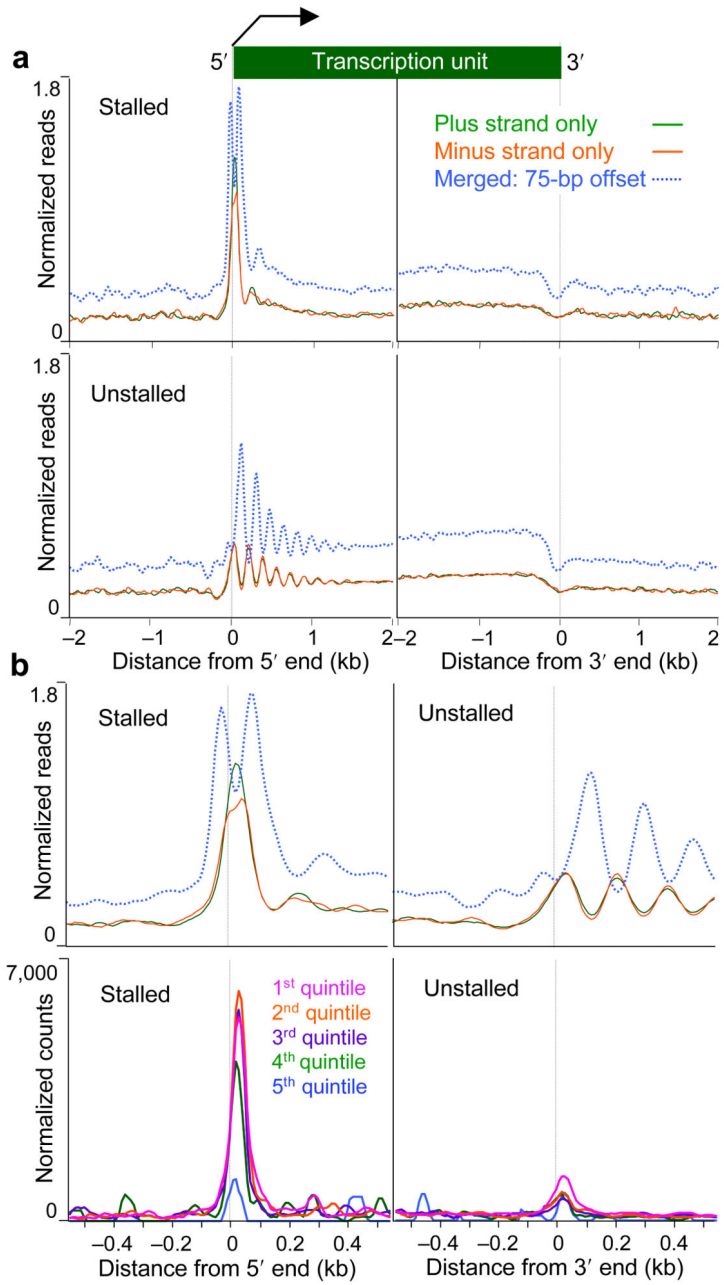

Figure 5.

Low-salt extracted chromatin reveals distinctive features of RNA Pol II stalling. Single-end sequence reads from DNA extracted from low-salt-soluble nucleosomes were displayed for 950 stalled and 4061 unstalled genes (**a**). The mapped ends of plus-strand reads were offset by adding 75 bp, and minus-strand reads were offset by subtracting 75 bp (dotted blue lines), which assumes that all reads represent one end or the other of a protected nucleosome core. Read ends were mapped separately for plus strands (green lines) and minus strands (orange lines) without offset, which assumes that all reads were derived from a small protected fragment. Average profiles are shown for low-salt-soluble nucleosomes mapped over genes in the stalled and unstalled classes. The *y*-axis refers to mapped single-end reads. As a

negative control, we also performed the same analysis at intron/exon junctions, but did not observe evidence of enhanced protection at the corresponding position in comparing stalled and unstalled profiles (Supplementary Fig. 10). (**b**) A biological replicate sample of low-salt extracted chromatin was subjected to limited paired-end sequencing. The 35–55-bp fraction is displayed in the bottom panels for quintiles of expression for genes in the stalled and unstalled classes. For comparison, the 5′ plots from panel (**a)** is shown in the panels above on the same *x*-axis scale. The *y*-axis refers to paired-end counts.

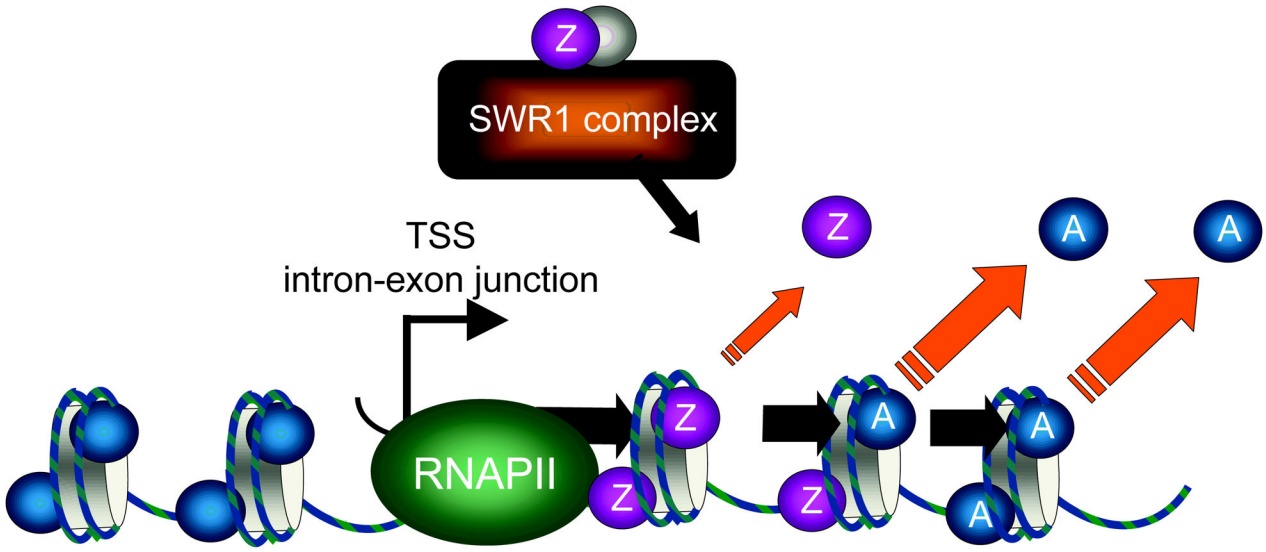

Figure 6.

Model for the generation of H2A.Z enrichment patterns. The cartoon depicts nucleosome disruptions that occur upon RNA Polymerase II transit. Pol II disruption causes dimer loss that is less for homotypic H2A.Z than for either heterotypic, or canonical H2A, with homotypic H2A.Z being the most stable nucleosome to disruption. H2A.Z homotypics are formed with multiple rounds of Pol II transit and remain relatively stable to further disruption. Heterotypics form but are relatively unstable to successive rounds of Pol II transit, leading to their depletion relative to homotypics. H2A.Z recruits remodelers which should exhibit the highest activity on homotypic H2A.Z, in support of transcription.